IEEE Access
Multidisciplinary | Rapid Review | Open Access Journal

Received 12 October 2022, accepted 4 November 2022, date of publication 14 November 2022, date of current version 18 November 2022.

Digital Object Identifier 10.1109/ACCESS.2022.3221954

RESEARCH ARTICLE

Improving the Robustness of the Dominant Mode Rejection Beamformer With Median Filtering

DAVID CAMPOS ANCHIETA AND JOHN R. BUCK, (Senior Member, IEEE)
Department of Electrical and Computer Engineering, University of Massachusetts Dartmouth, Dartmouth, MA 02740, USA
Corresponding author: David Campos Anchieta (danchieta@umassd.edu)

This work was supported by the Office of Naval Research under Award N00014-18-1-2415.

ABSTRACT Abraham's and Owsley's dominant mode rejection (DMR) beamformer modifies Capon's minimum variance distortionless response beamformer to force suitable constraints in the covariance matrix estimation process to reduce degrees of freedom. DMR estimates the ensemble covariance matrix (ECM) from a low-rank sample covariance matrix (SCM) by replacing the eigenvalues of the noise subspace with the sample mean of those same eigenvalues. This estimated noise power is negatively biased when the dominant subspace dimension is overestimated, which is common in practical implementations of the DMR. The proposed median DMR exploits the Marchenko-Pastur distribution to estimate the noise power from the median of the SCM eigenvalues. Simulations found that the median estimator was more robust to overestimating the dominant subspace dimension, exhibiting a lower mean squared error than the mean estimator. Simulations also found that the median DMR improves the white noise gain (WNG) when compared to the standard DMR in snapshot deficient scenarios with overestimated interferer subspace dimension. Higher WNG implies increased robustness to array perturbations. This work compares the median DMR to standard DMR in simulations with perturbed array element phase responses in a scenario with two interferers and background white noise. The median DMR preserved deeper notches than standard DMR in this scenario, increasing the output signal-to-noise ratio by roughly 1 dB.

INDEX TERMS Adaptive beamformer (ABF), dominant mode rejection (DMR), median filtering random matrix theory (RMT), sample covariance matrix (SCM).

I. INTRODUCTION

Hydrophone arrays permit both localizing the signal in the space (known as spatial filtering or beamforming) and suppressing background noise. The conventional beamformer (CBF) is the most straightforward array processor and the optimal beamformer in suppressing background white noise [1]. In passive sonar applications, loud interferers can overwhelm the CBF's spatial filtering ability and contaminate its output, masking the desired signal [1], [2]. Capon's minimum variance distortionless response (MVDR) adaptive beamformer (ABF) potentially prevents masking of the desired signal by creating destructive interference for the loud interferers, but the trade-off is reduced background white noise attenuation compared to the CBF [3]. The MVDR ABF inverts the ensemble covariance matrix (ECM) in the computation of the array weights for the beamformer.

The ECM is not available in most practical situations as it requires the knowledge of location and power of all the interferers. A common practical solution for this impasse is to perform a sample matrix inversion (SMI) with a sample covariance matrix (SCM) estimated from snapshots of data [1]. This solution requires that the number of snapshots exceeds the number of sensors in the array so the resulting sample covariance matrix (SCM) is invertible. Also, the SMI MVDR may require twice as many snapshots as the number of sensors to achieve half of the signal to noise ratio performance of the ensemble MVDR [4]. Acquiring enough snapshots for an invertible and accurate estimate of the covariance matrix may be impractical for large arrays or environments with moving interferers, so a reduced degrees of freedom ABF may be necessary in those situations.

The associate editor coordinating the review of this manuscript and approving it for publication was Chengpeng Hao.

The dominant mode rejection (DMR) ABF reduces the degrees of freedom of the MVDR beamformer by constraining the smallest eigenvalues of the SCM to be equal, allowing for an approximation of the ECM with fewer snapshots [5]. Each of the large eigenvalues of the SCM (and its respective eigenvector) is generally associated with one loud interferer to be attenuated. Together, these eigenvectors form a basis for the interferer, or dominant, subspace. The remaining small eigenvalues are replaced with an estimate of the background noise power equal to their sample mean, as they are assumed to belong to the noise subspace. Many other ABFs impose constrains on the SCM to regularize the array weights [6], [7], [8], [9], [10]. In this paper, we focus on the dominant mode rejection ABF.

A correct choice of the dimension of the dominant subspace in the DMR beamformer is important to ensure interferer and noise attenuation. Practical implementations of the DMR often overestimate the number of interferers [11], [12]. Overestimating the number of interferers is the safely conservative choice, because this approach guarantees that no loud interferer will pass unattenuated. The downside of this approach is that it reduces the number of eigenvalues averaged to estimate the noise power. The resulting estimator is less precise and negatively biased. The noise estimate is less precise in this case because averaging fewer eigenvalues results in a larger variance for the estimate than the variance when the subspace rank is correct. The noise estimate is negatively biased because the eigenvalues removed from the average are always the largest eigenvalues of the noise subspace. The negative bias estimating the noise power also degrades the ability of the beamformer to attenuate background noise.

This paper proposes a modification to the DMR beamformer to estimate the noise power as a function of the median of the nonzero eigenvalues of the SCM. The median was chosen for its known robustness against outliers and truncation of data [13], [14]. This robustness makes the estimator unbiased if the actual number of interferers is less than half of the number of snapshots used in the computation of the SCM. The relationship between the sample median of the eigenvalues and the noise power was derived from a linear regression on numerical evaluations over the Marchenko-Pastur (MP) probability function [15]. The median estimator also has the advantage of not being dependent on the estimated number of interferers.

For the past 30 years, several researchers studied and improved the DMR beamformer. Cox added mismatch protection to avoid the suppression of a desired signal slightly off the steering direction [16]. Redheendran and Gramann evaluated the performance of the DMR with real world array data and demonstrated that the DMR achieves similar performance to other ABFs but with a shorter integration time [11], [12]. Wage and Buck investigated how the DMR beamformer performance converges as a function of snapshots and interferer power [2], [17], [18], [19]. Santos et al. proposed a parametric estimation of the ECM that includes a noise power estimate based on order statistics [20], which is comparable to what this paper proposes, but does not exploit random matrix theory results.

The paper is organized as follows. Section II presents a brief theoretical background on array signal processing and establishes the notation of this paper. Section III explains the Marchenko-Pastur distribution of the eigenvalues of SCMs and derives an estimator of the noise power based on the sample median of those eigenvalues. Section IV evaluates the performance of the median DMR compared to the standard DMR, as well as the quality of the noise power estimators for different number of snapshots and dominant subspace dimension. Section V extends the comparison to the more practical case where the array suffers from phase perturbations due to array element location errors or sensor calibration errors. Finally, Section VI discusses the results and draws conclusions.

II. BACKGROUND

This section summarizes the necessary background on beamforming, including the performance metrics and the DMR implementation used in this paper. Most of the theory presented in this section is summarized from [1] with notation aligned with that in [2].

A. SIGNAL MODEL

A narrowband plane wave arrives at a uniform linear array (ULA) with a constant time delay from sensor to sensor that is a function of the angle of arrival θ. In the frequency domain, this time delay translates to a complex phasor that multiplies the complex magnitude of the plane wave. A plane wave with angle of arrival θ_i is associated with a replica vector:

$$\begin{aligned} \mathbf{v}_i &= \mathbf{v}(u_i) = [\exp(jz_1k_0u_i), \ldots, \exp(jz_Nk_0u_i)]^T, \\ u_i &= \cos(\theta_i), \\ k_0 &= 2\pi/\lambda, \end{aligned} \tag{1}$$

where λ is the wavelength and z_n is the position of the n-th sensor on the z-axis.

The phasors of the narrowband data vector ($\mathbf{x}$) are the Fourier transform of the sensor measurements evaluated at the carrier frequency [1]. Those measurements are assumed to result from the sum of planewaves $\mathbf{v}_i$ plus background white noise $\mathbf{n}$:

$$\begin{aligned} \mathbf{x} &= \sum_{i=1}^{D_{\text{true}}} \mathbf{v}_i a_i + \mathbf{n} \\ \mathbf{n} &\sim \mathbb{CN}(\mathbf{0}, \sigma_n^2\mathbf{I}) \\ a_i &\sim \mathbb{CN}(0, \sigma_i^2), \end{aligned} \tag{2}$$

where D_{true} is number of waves arriving on the array; $\mathbf{v}_i$, a_i, and σ_i^2 are respectively the replica vector, complex amplitude, and power of the i^{th} plane wave. The power of background white noise is σ_n^2.

In the frequency domain, a beamformer is represented by an inner product of the array weights $\mathbf{w}$ with the data vector $\mathbf{w}^H\mathbf{x}$. Each complex phasor in $\mathbf{w}$ represents the frequency

response of a filter applied to the corresponding sensor measurement before summing across the array.

The conventional beamformer (CBF) is the most straightforward beamformer. The CBF is a spatial matched filter for planewaves arriving from the direction described by the steering vector $\mathbf{v}_s$:

$$\mathbf{w}_{\text{CBF}} = \tfrac{1}{N}\mathbf{v}_s. \tag{3}$$

The CBF works well in scenarios with white background noise and interferers not much louder than the desired signal. However, the spatial filtering ability of the CBF may not be enough to suppress loud interferers. An ABF may be necessary in those situations to prevent masking of the desired signal.

B. DMR BEAMFORMER

The dominant mode rejection (DMR) is an ABF that modifies Capon's minimum variance distortionless response beamformer (MVDR) to work with fewer degrees of freedom and thus with fewer snapshots of data [5]. The weights of the DMR beamformer are a function of the sample covariance matrix of the measured data, defined by:

$$\mathbf{S} = \frac{1}{K}\sum_{k=1}^{K}\mathbf{x}_k\mathbf{x}_k^H. \tag{4}$$

Assuming that the observed data contains D loud interferers, the DMR decomposes the SCM into its eigenvalues and eigenvectors and separates them into two subspaces:

$$\mathbf{S} = \overbrace{\sum_{i=1}^{D} g_i\mathbf{e}_i\mathbf{e}_i^H}^{\text{interferers}} + \overbrace{\sum_{i=D+1}^{N} g_i\mathbf{e}_i\mathbf{e}_i^H}^{\text{noise}}, \tag{5}$$

where g_i are the eigenvalues, $\mathbf{e}_i$ are the eigenvectors, and $g_1 \geq g_2 \geq \cdots \geq g_N$. The D largest eigenvalues are associated with the loud interferers, while the smallest ones belong to the noise subspace. If $K < N$, then the $N - K$ smallest eigenvalues $g_{K+1}, \ldots, g_N$ will be zero. The DMR then replaces the sample eigenvalues of the noise subspace with an estimate of the noise power s_n^2:

$$\mathbf{S}_{\text{DMR}} = \sum_{i=1}^{D} g_i\mathbf{e}_i\mathbf{e}_i^H + s_n^2\sum_{i=D+1}^{N}\mathbf{e}_i\mathbf{e}_i^H. \tag{6}$$

The DMR inverts this modified SCM to calculate the array weights just like MVDR:

$$\mathbf{w}_{\text{DMR}} = \frac{\mathbf{S}_{\text{DMR}}^{-1}\mathbf{v}_s}{\mathbf{v}_s^H\mathbf{S}_{\text{DMR}}^{-1}\mathbf{v}_s}. \tag{7}$$

Traditional implementations of the DMR use a noise power estimate based on the average of the eigenvalues of the noise subspace $[g_{D+1}, \ldots, g_N]$. However, this paper evaluates snapshot deficient cases (i.e. $K < N$), in which the eigenvalues $[g_{K+1}, \ldots, g_N]$ are zero and deterministic. Henceforth, whenever this paper mentions *standard DMR*, it refers to the DMR described by (6) and (7) with noise power estimator based on the sample mean of the nonzero eigenvalues only $[g_{D+1}, \ldots, g_K]$:

$$s_n^2 = \frac{K}{N}\left(\frac{1}{K-D}\right)\sum_{i=D+1}^{K} g_i. \tag{8}$$

The expectation of the nonzero eigenvalues is $\sigma_n^2 N/K$ [15], hence the need to multiply their sample mean by K/N to correct for this bias.

The performance of the DMR converges with fewer snapshots when compared to the SMI MVDR. Wage and Buck demonstrated through simulations that the signal to interferer and noise ratio (SINR) loss of the DMR is beta distributed [19]. However, the distribution of the SINR of DMR doesn't depend on the number of sensors N. Rather it depends on K and D. The DMR requires $K \cong 2D$ snapshots to achieve half of the SINR of the ensemble MVDR [21].

In practice, the actual number of interferers D_{true} is unknown and the dominant signal subspace dimension D is an estimate from the observed data. Choosing the dominant signal subspace dimension can be a challenging model-order selection problem. Incorrectly choosing D biases the noise power estimate s_n^2, as discussed in more detail in Section III.

C. PERFORMANCE METRICS

The beampattern is the complex gain of a specific array weight vector to plane waves as a function of the angle of arrival. The squared magnitude of the beampattern is the power pattern:

$$|\text{B}(u)|^2 = |\mathbf{w}^H\mathbf{v}(u)|^2. \tag{9}$$

The notch depth (ND) is the power pattern in the direction of strong interferers [2]:

$$\text{ND}_i = |\text{B}(u_i)|^2 = |\mathbf{w}^H\mathbf{v}_i|^2. \tag{10}$$

Adaptive beamformers like DMR and MVDR are designed to have a power pattern close to zero in the direction of loud interferers. The ND decreases as a function of the interferer to noise ratio $\text{INR}_i = \sigma_i^2/\sigma_n^2$. For low INR, the ND will be equal to the response of the CBF ($\text{ND}_i = |\mathbf{v}_s^H\mathbf{v}_i|^2/N^2 = \cos^2(\mathbf{v}_s, \mathbf{v}_i)$). Once $\text{INR}_i \gg 1/N \sin^2(\mathbf{v}_s, \mathbf{v}_i)$ the notch depth in dB is

$$10\log_{10}\text{ND}_i = O(-20\log_{10}\text{INR}_i), \tag{11}$$

i.e., it decreases with slope -2 as a function of the INR expressed in dB [17]. The squared generalized sine between vectors $\sin^2(\mathbf{v}_s, \mathbf{v}_i)$ is described in Section II.A of [22].

The output power (OP) of the interferers measures the ability of a beamformer to attenuate a particular set of interferers and is directly related to the notch depth:

$$\text{OP}_{\text{interf}} = \sum_{i=1}^{D_{\text{true}}}\sigma_i^2|\mathbf{w}^H\mathbf{v}_i|^2 = \sum_{i=1}^{D_{\text{true}}}\sigma_i^2\text{ND}_i. \tag{12}$$

From (11) one can say that, in an ideal scenario without mismatch in the location of interferers, the notch depth of

an ABF to a loud interferer is $\mathrm{ND}_i = O((\sigma_i^2)^{-2})$. Thus, the output power due to an individual interferer is $O((\sigma_i^2)^{-1})$, i.e., the interferer with the lowest input power among the loud interferers tend to contribute the most power to the beamformer output (12).

The white noise gain (WNG) is a measure of how much the array improves the signal-to-noise ratio (SNR) [1], for a single planewave in white noise. For an array weight vector $\mathbf{w}$ with unity gain at steering direction, the WNG is:

$$\mathrm{WNG} = \frac{1}{\mathbf{w}^H\mathbf{w}}. \tag{13}$$

The WNG is also inversely proportional to the sensitivity of the beamformer to sensor location errors [23]. The CBF achieves the optimal WNG N, which is equal to the number of sensors in the array.

The output signal to interferer and noise ratio (SINR) is a function of both the WNG and the output power of the interferers. The SINR measures how well the filter attenuates background noise and interferers in favor of the signal:

$$\begin{aligned}\mathrm{SINR} &= \sigma_s^2(\mathbf{w}^H\boldsymbol{\Sigma}\mathbf{w})^{-1} \\ &= \sigma_s^2\left(\mathrm{OP}_{\mathrm{interf}} + \sigma_n^2/\mathrm{WNG}\right)^{-1},\end{aligned} \tag{14}$$

where σ_s^2 is the power of the signal of interest, and $\boldsymbol{\Sigma}$ is the ECM of noise plus interferers. Capon's MVDR beamformer with inversion of the ECM optimizes the output SINR [1].

The mean squared error (MSE) measures the performance of the noise power estimator. The MSE equals the bias squared plus the variance of the estimator [24]:

$$\mathrm{mse}\left(s_n^2\right) = \left(E\left\{s_n^2\right\} - \sigma_n^2\right)^2 + \mathrm{Var}\left[s_n^2\right]. \tag{15}$$

Maintaining a small MSE while overestimating the dominant subspace dimension and suffering from array element perturbations indicates robust performance for the DMR beamformer.

D. EXPECTED POWER PATTERN OF ARRAYS WITH PHASE PERTURBATIONS

Array phase perturbations can be especially degrading to the interferer attenuation of ABFs, but have negative effects on the performance of any beamformer. Phase perturbations are a result of mismatch between the actual position of the sensors and the nominal position (used to calculate the steering vector). These perturbations can also be caused by variations in the phase response of amplifiers and filters in the physical array.

The phase perturbation is represented by a random phase shift applied to the measurements of each sensor:

$$\begin{aligned}\mathbf{x}_{\mathrm{pert}} &= \mathbf{x} \odot [e^{j\Delta\phi_1}, e^{j\Delta\phi_2} \ldots, e^{j\Delta\phi_N}]^T \\ \Delta\phi_n &\sim \mathcal{N}(0, \sigma_\phi^2).\end{aligned} \tag{16}$$

where $\odot$ is the Hadamard (element-wise) product. Note that the phase perturbation is assumed to be uncorrelated in both space (sensor to sensor) and time (snapshot to snapshot).

In principle, random phase perturbations may wrap around periodically every 2π, requiring the use of the Von Mises distribution, or wrapped normal [25], [26]. In practice, this paper focuses on cases with relatively small perturbations ($\sigma_\phi \leq \pi/5$). Phase errors large enough to "wrap around" are very improbable.

The phase perturbation affects the expected power pattern in two ways: slightly attenuating the desired beampattern and, more importantly when nulling interferers, filling in the notches. Gilbert and Morgan derived the expected power pattern of arrays with element perturbations [1], [23]:

$$E_{\boldsymbol{\phi}}\{|B(u)|^2\} = |B^{(n)}(u)|^2 \exp[-\sigma_\phi^2] + \|\mathbf{w}\|^2\sigma_\phi^2, \tag{17}$$

where $B^{(n)}(u)$ is the beampattern of nominal (unperturbed) weights. The $E_{\boldsymbol{\phi}}$ with subscript $\boldsymbol{\phi}$ means that the expectation is integrated over the possible sets of perturbations $[\Delta\phi_1, \ldots, \Delta\phi_N]$. In addition, the expectation in (17) presumes a deterministic array of weights $\mathbf{w}$. However, the weights of the DMR are random, since they depend on the set of random snapshots of data. Therefore, the actual expected beampattern of perturbed arrays is the result of a nested expectation that integrates over both snapshots and perturbations:

$$E_{\boldsymbol{\phi},\mathbf{w}}\{|B(u)|^2\} = E_{\mathbf{w}}\left\{E_{\boldsymbol{\phi}}\{|B(u)|^2|\mathbf{w}\}\right\}. \tag{18}$$

In the asymptotic region of sufficiently loud interferers, the perturbed notch depth depends only on the variance of the perturbation and the white noise gain, not on the nominal notch depth [23]. For sufficiently large INR_i, the notch depth of the DMR power pattern $|B^{(n)}(u)|^2$ will be below $|\mathbf{w}_{\mathrm{DMR}}|^2\sigma_\phi^2$, so the second term will dominate (17). The resulting notch depth for the ABF on the perturbed array is:

$$\begin{aligned}10\log_{10}\mathrm{ND} &= 10\log_{10}\sigma_\phi^2 + 10\log_{10}\|\mathbf{w}\|^2 \\ &= 10\log_{10}\sigma_\phi^2 - 10\log_{10}(\mathrm{WNG}).\end{aligned} \tag{19}$$

This result contrasts with the inferences developed in Section II-C regarding notch depth and output power of interferers. From (19) we see that the perturbed ND will be about the same for all interferers given that nominal ND is low enough. As a result, the output power from interferers increases during mismatch, with loud interferers contributing with the most power, in contrast to the ensemble case discussed earlier where the weaker interferers contribute with the most power.

ABFs with higher WNG will have deeper notches in their beampatterns for perturbed arrays, thus are less sensitive to array phase perturbations. Improving the SCM estimation increases WNG while preserving the deep notches of an ABF [21], [27].

III. THE MEDIAN-BASED ESTIMATOR OF THE NOISE POWER

Practical ABFs estimate the ECM by averaging the outer products of K snapshots of noisy data, as described in (4).

The eigenvalues g_i of the SCM are random variables themselves. When the snapshots only contain background noise, the SCM is a Wishart matrix and the eigenvalues behavior is well-modeled by by the Marchenko-Pastur (MP) distribution [15], [28], [29]. When the snapshots contain a few strong interferers plus background noise, the MP distribution still accurately models the distribution of the eigenvalues in the noise subspace. This distribution has two parameters: the noise power, which is also the expectation of the eigenvalues, $\sigma_n^2 = \mathrm{E}\{g_i\}$; and the sensors per snapshot ratio $C = N/K$. The distribution also has a limited region of support $\sigma_n^2(1 - \sqrt{C})^2 < g_i < \sigma_n^2(1 + \sqrt{C})^2$, which becomes wider when either C or σ_n^2 increases.

When there are loud interferers in the environment, the eigenvalues of the interferer subspace have a positive bias and should be disregarded when estimating the noise power. This is why the standard DMR uses the average of the eigenvalues of the noise subspace of the SCM as the estimator of the noise power [16]. The parameter D of the DMR defines how many interferers need suppression and which eigenvalues will be averaged in the computation of s_n^2. DMR eliminates the first D eigenvalues from the noise power estimate to avoid bias and ensure suppression of the loud interferers. When the actual number of interferers D_{true} is unknown, D is often conservatively, and deliberately, overestimated [11], [12]. Overestimation is chosen because underestimating the dominant subspace dimension causes leaking of interferers and bias to the noise power estimate that harm the SINR and WNG of the DMR. On the other hand, overestimating the dominant subspace dimension introduces a negative bias in the noise power estimate and reduces its precision, since the estimate is the average of fewer and smaller eigenvalues. On balance, the small decrease in SINR caused by overestimating D and reducing the WNG is safer than the risk of a large SINR decrease that results when D underestimates the number of interferers.

Median filtering and order statistics are more robust than the sample mean against impulsive noise and outliers in data [13], [14]. To develop the median-based estimator of the noise power in snapshot deficient scenarios, we analyzed the cumulative density function (CDF) of the nonzero eigenvalues of the standard ($\sigma_n^2 = 1$) Marchenko-Pastur distribution to find a relationship between the ensemble median and the parameter C. Figure 1 plots contours of this CDF for rank deficient sample covariance matrices ($C > 1$) against the random variable g and the parameter C [15]. The median nonzero eigenvalue median$[g]$ for each C is the value of g satisfying $F(g; C) = 0.5$. The $F(g; C) = 0.5$ contour is very closely approximated by a linear regression $g = (C - 0.345)$, as shown in Figure 1. The contour plot in Figure 1 shows that the ensemble median can be approximated by a linear regression as a function of C. Scaling properties of eigenvalues, moments and order statistics extends this regression for nonstandard ($\sigma_n^2 \neq 1$) MP distributions, yielding

$$\text{median}[g] = \sigma_n^2(C - 0.345). \tag{20}$$

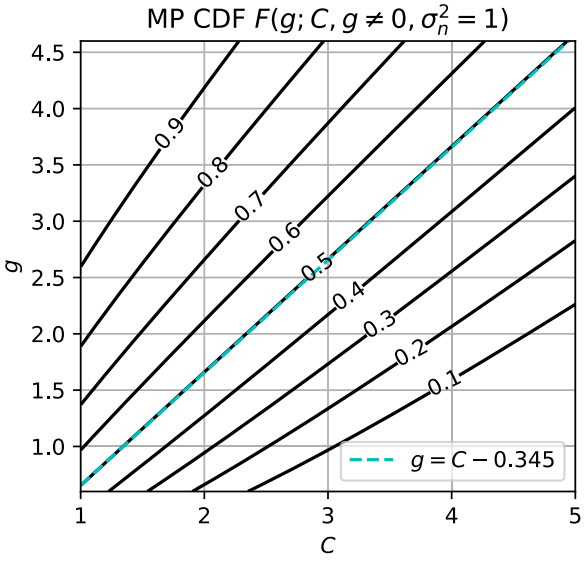

FIGURE 1. Contour plot of the standard ($\sigma_n^2 = 1$) CDF of the nonzero eigenvalues of Wishart SCM versus the random variable g and parameter C for the rank deficient ($C > 1$) case. The relationship between the median of the nonzero eigenvalues and C is accurately approximated by the linear regression (dashed cyan line).

Rearranging those terms derives the median-based estimator of the noise power

$$s_n^2 = \text{median}[g_1, \ldots, g_K]/(C - 0.345), \tag{21}$$

where median$[g_1, \ldots, g_K]$ is the sample median of the nonzero eigenvalues of the low-rank SCM obtained by averaging the outer products of K snapshots.

A power estimate based on the mean of the $K - D$ smallest nonzero eigenvalues will be biased if there is any error in D. If D is too small, "interferer" eigenvalues will be included in the average, creating a positive bias in s_n^2. If D is too large, then the larger "noise" eigenvalues will be omitted from the average, creating a negative bias in s_n^2.

In contrast with the mean estimator, the median based estimator is insensitive to the choice of D. The sample median is computed from all K nonzero sample eigenvalues without regards to D. Therefore, the sample median power estimator is only impacted in the extreme scenario that the true number of interferers D_{true} exceeds half of the number of snapshots K. In this scenario, the noise power estimate will be biased since the median will be an interferer eigenvalue. Despite the median estimator being insensitive to D, the chosen dominant subspace dimension still determines which eigenvalues will be replaced in the modified covariance matrix in (6).

IV. PERFORMANCE OF THE MEDIAN DMR

This section compares the performance of the median DMR with the standard DMR while varying the assumed dominant subspace dimension D and the number of snapshots K. The simulated ULA has $N = 51$ sensors with half-wavelength spacing. All results are based on 1000 Monte Carlo simulations. The metrics used to evaluate the performance of

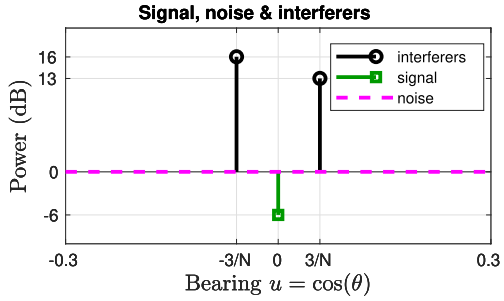

FIGURE 2. Scenario describing the powers and locations of the signal and interferers as well as the noise floor. Although the domain of u contains all real values from -1 to 1, the horizontal axis is truncated to better show the signals of interest.

the beamformers were the output SINR, the WNG, and the estimated input noise power s_n^2.

Figure 2 illustrates the simulated scenario, which included two loud interferers (13 dB and 16 dB INR) located in the direction of the highest side lobes of the conventional beamformer ($u = \pm 3/N$). Both the noise and interferers are louder than the desired signal located at broadside ($u = 0$) with signal-to-noise ratio of -6 dB. The CBF does not have enough interferer attenuation for this scenario, hence an ABF like the MVDR is necessary to find the desired signal.

Despite having a higher variance, the median-based estimator of the noise power retains a lower bias than the mean-based estimator when the interferer subspace dimension is overestimated. Figure 3 compares the accuracy and precision of both estimators of noise power as a function of the number of snapshots and interferer subspace dimension D. The value of D ranges from correct $D = D_{\text{true}} = 2$ to highly overestimated $D = 11$ and $D = 23$, while the number of snapshots ranges from highly deficient $K = 6$ to almost full rank $K = 48$. As expected, the bias of the mean estimator (plotted in red circles) increases rapidly as the dominant subspace dimension is overestimated, increasing the mean squared error (MSE) even though the variance is lower. Overestimating the dominant subspace dimension necessarily eliminates the highest noise eigenvalues from the sample mean computation, increasing the bias squared. On the other hand, the bias of the median-based estimator (blue stars) is not affected by the increase in D, showing that the median estimator itself does not depend on the chosen dominant subspace dimension. Also, the bias of the median-based estimator approaches zero as K increases, suggesting that the estimator is asymptotically unbiased.

Figure 4 compares the performance metrics of both the standard DMR and median DMR. The plots on the first row show the output SINR, the plots on the second row show WNG, and the plots on the third row show the total output power contributed by the interferers. Each column is associated with a value of D indicated on top of each plot. For all plots, the number of snapshots is on the horizontal axis, while the performance metric is on the vertical axis. The red symbols indicate the performance metric of the standard

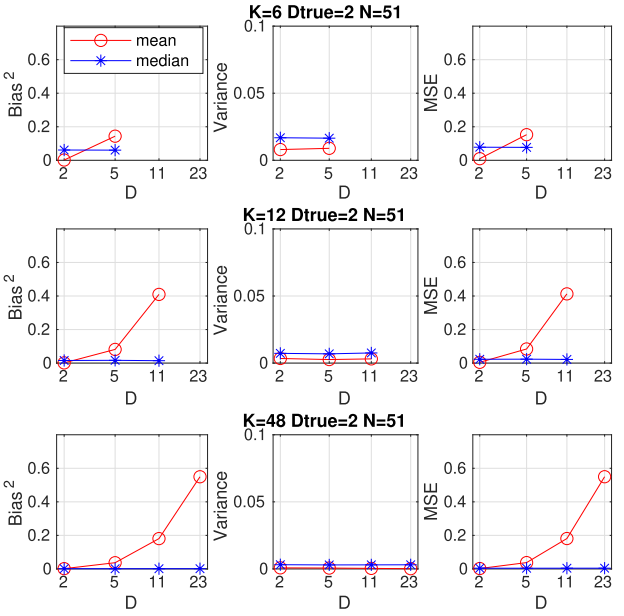

FIGURE 3. Bias, variance and mean of squared error (MSE) of the median-based estimator of the noise power compared to the mean-based estimator as a function of number of snapshots and estimated interferer subspace dimension. Each point is an average over 1000 Monte Carlo trials of Wishart matrix of the scenario presented in Figure 2 Despite having a higher variance, the median-based estimator has a lower bias than the mean-based estimator when the number of interferers is overestimated. Note that the figure plots the variance in a different scale than that of the bias squared and MSE.

DMR averaged over 1000 Monte Carlo trials, while the blue symbols do the same for the median DMR. The vertical intervals contain 90% of the results. The green line shows the performance for the optimal adaptive beamformer, which is the MVDR with ensemble covariance matrix.

The difference in performance between median DMR and standard DMR increases with overestimation of dominant subspace dimension D, with the median DMR preserving better and more consistent performance. The metrics with $D = 5$, shown in the leftmost column of Figure 4, show that the difference in performance between the standard and median DMR is very small when D is closer to the real number of loud interferers $D_{\text{true}} = 2$. For $D = 11$, shown in the middle column, the performance for both standard and median DMR decreases when compared to the $D = 5$ case. However, the decrease in the performance of standard DMR is greater, increasing the difference between standard and median DMR. The rightmost column of Figure 4 shows the performance of DMR when the dominant subspace dimension $D = 23$ is highly overestimated. This case yields the largest difference in performance between the standard DMR and the median DMR. For the $D = 23$ case, the larger values of the blue symbols in the SINR and WNG plots, and the smaller confidence intervals for those values, indicate that median DMR is more robust against overestimation of the dominant subspace dimension.

The output power of interferers, shown in the third row of Figure 4, decreases more with increasing snapshots K

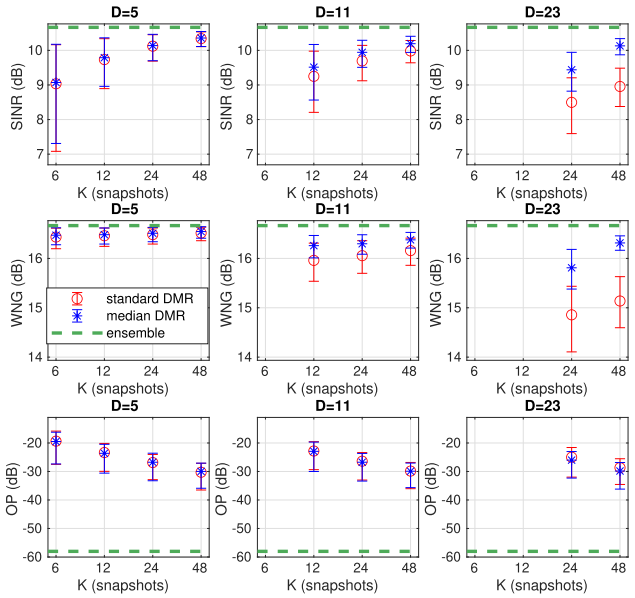

FIGURE 4. Average performance metrics of the standard DMR (red circles) and the median DMR (blue stars) over 1000 Monte Carlo simulations as a function of the number of snapshots K and the estimated number of interferers D. The vertical lines cover the 90% confidence intervals. The green line plots the performance of the MVDR with ensemble covariance matrix, which is the optimal ABF. All the metrics are impacted by the overestimation of D, but the median DMR preserves a higher WNG and SINR, and a lower interferer contribution to output power as the dominant subspace dimension D increases.

TABLE 1. Average notch depth of both DMR beamformers at the angles of the interferer.

ND (dB)	u_1	u_2
Standard DMR	-25.05	-25.00
Median DMR	-26.19	-26.15

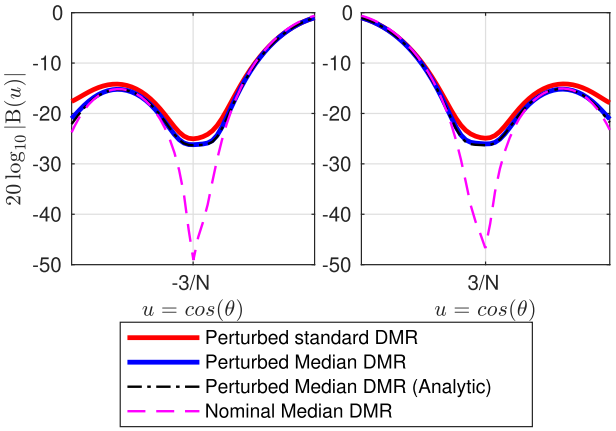

FIGURE 5. Average power pattern of perturbed standard DMR, perturbed median DMR, nominal median DMR, and expected (analytic) perturbed median DMR, as a function of u, at the region of the loud interferers. The phase perturbation raises the notches of both standard DMR and median DMR, but the median DMR preserves deeper notches than the standard DMR. The black dashed line follows the blue line very closely, meaning that the analytic expression by Gilbert and Morgan accurately predicts the simulation results.

than it grows with increasing subspace dimension D for both standard DMR and median DMR. For median DMR, the output power contributed by interferers is essentially unchanged as D increases, demonstrating the anticipated robustness. In contrast, the standard DMR output power contributed by interferers increases by about 1.1 dB relative to the median DMR for the $D = 23$ $K = 48$ case. However, since the output power of interferers is very small relative to the white noise contribution to the output noise power in both cases, the small improvement has little impact in the overall SINR.

V. PERFORMANCE OF THE MEDIAN DMR AGAINST PHASE PERTURBATION IN ARRAYS

This section tests the median DMR against array element perturbations through Monte Carlo simulations and compares its performance to Gilbert and Morgan's analytic expression presented in Section II-D. The results in the previous section show that the median DMR has some performance improvement when the beamformers highly overestimated the dominant subspace dimension D. Most of this gain in SINR of the median DMR is due to the improvement in WNG. Recall that WNG is inversely proportional to the norm squared of the array weight vector $\|\mathbf{w}\|^2$ (13), while the sensitivity of the notch depths are directly proportional to this quantity (17). Since the WNG of the median DMR is about 1 dB higher than that of the standard DMR, equation (19) predicts that in arrays with phase perturbations, the nulls of the beampattern of the median DMR will be 1 dB deeper than those of the standard DMR. The deeper notch reduces the interferer contribution to output power, which improves the SINR.

The simulated scenario is the same of Section IV with respect to number of sensors, interferers, background noise, and signal. The phase perturbation has a standard deviation of $\sigma_\phi = \sqrt{0.1}$ radians. This perturbation is comparable to a standard deviation of about $\lambda/20$ of random error in the array sensor positions.

As discussed in Section II-D, Gilbert and Morgan's expected beampattern of perturbed arrays in (17) assumes deterministic weights and nominal beampattern, which is not the case for the DMR. Consequently, this work uses nested Monte Carlo trials in order to implement the nested expectation in (18). A total of 1800 simulations were run for both perturbed and unperturbed arrays. These simulations contained 30 independent realizations of K snapshots with an unperturbed array to estimate the expected nominal beampattern for both standard and median DMR. This nominal beampattern and weight were passed as arguments to (17) to obtain the analytic result for the perturbed beampattern. Each of the 30 realizations of snapshots was then perturbed with 60 independent realizations of the array phase errors, resulting in 1800 samples of the perturbed DMR array weights. As shown in (18), the combined effect should converge to the same result as randomizing both phase errors and snapshots simultaneously. Structuring the Monte Carlos as nested loops implementing the conditional expectations permits us

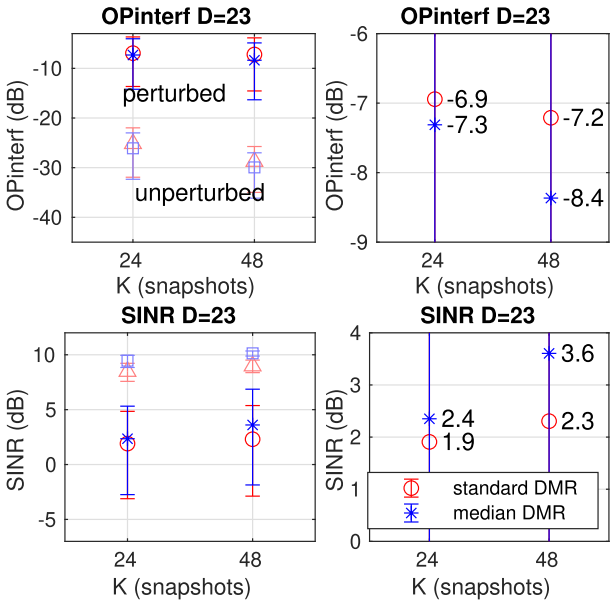

FIGURE 6. Average interferer contribution to output power and SINR on perturbed arrays for the standard DMR beamformer (red symbols) and median DMR beamformer (blue symbols) when $D = 23$. The lighter symbols in the leftmost plots show the DMR performance on unperturbed arrays for comparison. The perturbations harm the interferer attenuation of both DMR beamformers increasing the interferer contribution to output power and decreasing the SINR as shown in the left column of plots. However, the median DMR is more robust to array perturbations, consistently attenuating the interferers more and improving SINR.

to leverage Gilbert and Morgan's analytic results for perturbed power patterns as well.

Figure 5 compares the notches of standard DMR and median DMR in the direction of the two loud interferers for the case with $D = 23$ and $K = 48$, which is the one that showed the most improvement in WNG in the unperturbed case. The red lines plot the average power pattern of the perturbed standard DMR beamformer. The blue lines plot the average power pattern of the perturbed median DMR. The dashed magenta line is the mean power pattern of the nominal median DMR without perturbations. The black dashed line shows the expected power pattern of the perturbed median DMR predicted by evaluating the nominal power pattern in (17). The power pattern of the median DMR has slightly deeper notches in the direction of strong interferers. Table 1 displays the average value of those notches. The notches of median DMR are on average about 1.1 dB deeper than those of the standard DMR. The proximity between the black dashed line and the blue solid line in Figure 5 confirms that the result in (17) accurately predicts the notch depth of the DMR beamformer for the perturbed array.

Figure 6 compares the SINR and the interferer contribution to output power of the phase perturbed median DMR and standard DMR for the large subspace dimension ($D = 23$). The left column of plots compares the performance of the unperturbed array (lighter symbols) with the perturbed array (darker symbols). The phase perturbations impaired the interferer attenuation of the DMR causing a higher interferer contribution to output power and lower SINR. The right column of plots zooms in on the perturbed array performance. Although the phase perturbations affected the performances of both DMRs, the median DMR, shown by the blue symbols, preserved lower output power due to interferers and higher SINR than the standard DMR.

VI. CONCLUSION

This paper proposes and evaluates the median DMR beamformer, a modification to the DMR ABF that estimates the power in the noise subspace as a function of the median rather than the mean of specific sample eigenvalues.

The median-based estimator makes the DMR ABF more robust to errors in estimating interferer subspace dimension in a typical passive sonar scenario. Simulations demonstrate that the median-based estimator has lower MSE than the mean-based estimator for DMR with highly overestimated interferer subspace dimension. The reduced MSE of the median-based estimator is mainly due to reduced bias, even though the sample median has higher variance when compared to the sample mean estimator.

Median DMR's improved performance is primarily due to higher WNG. The improved WNG also results in better performance for median DMR when challenged by perturbed arrays, consistent with the predictions of Gilbert & Morgan's model.

REFERENCES

[1] H. L. V. Trees, *Detection, Estimation, and Modulation Theory: Part IV*. Hoboken, NJ, USA: Wiley, 2005.
[2] K. E. Wage and J. R. Buck, "Snapshot performance of the dominant mode rejection beamformer," *IEEE J. Ocean. Eng.*, vol. 39, no. 2, pp. 212–225, Apr. 2014.
[3] J. Capon, "High-resolution frequency-wavenumber spectrum analysis," *Proc. IEEE*, vol. 57, no. 8, pp. 1408–1418, Aug. 1969.
[4] I. S. Reed, J. D. Mallett, and L. E. Brennan, "Rapid convergence rate in adaptive arrays," *IEEE Trans. Aerosp. Electron. Syst.*, vol. AES-10, no. 6, pp. 853–863, Nov. 1974.
[5] D. A. Abraham and N. L. Owsley, "Beamforming with dominant mode rejection," in *Proc. Conf. Eng. Ocean Environ.*, Washington, DC, USA, Sep. 1990, pp. 470–475.
[6] P. Stoica, H. Li, and J. Li, "A new derivation of the APES filter," *IEEE Signal Process. Lett.*, vol. 6, no. 8, pp. 205–206, Aug. 1999.
[7] A. Aubry, A. De Maio, and V. Carotenuto, "Optimality claims for the FML covariance estimator with respect to two matrix norms," *IEEE Trans. Aerosp. Electron. Syst.*, vol. 49, no. 3, pp. 2055–2057, Jul. 2013.
[8] S. R. Tuladhar and J. R. Buck, "Unit circle rectification of the minimum variance distortionless response beamformer," *IEEE J. Ocean. Eng.*, vol. 45, no. 2, pp. 500–510, Apr. 2020.
[9] B. D. Carlson, "Covariance matrix estimation errors and diagonal loading in adaptive arrays," *IEEE Trans. Aerosp. Electron. Syst.*, vol. AES-24, no. 4, pp. 397–401, Jul. 1988.
[10] D. Fuhrmann, "Application of Toeplitz covariance estimation to adaptive beamforming and detection," *IEEE Trans. Signal Process.*, vol. 39, no. 10, pp. 2194–2198, Oct. 1991.
[11] T. Messerschmitt and R. Gramann, "Evaluation of the dominant mode rejection beamformer using reduced integration times," *IEEE J. Ocean. Eng.*, vol. 22, no. 2, pp. 385–392, Apr. 1997.
[12] T. M. Redheendran and R. A. Gramann, "Initial evaluation of the dominant mode rejection beamformer," *J. Acoust. Soc. Amer.*, vol. 104, no. 3, pp. 1331–1344, Sep. 1998.
[13] A. C. Bovik, T. S. Huang, and D. C. Munson, "A generalization of median filtering using linear combinations of order statistics," *IEEE Trans. Acoust., Speech, Signal Process.*, vol. ASSP-31, no. 6, pp. 1342–1350, Dec. 1983.

[14] P. P. Gandhi and S. A. Kassam, "Analysis of CFAR processors in nonhomogeneous background," *IEEE Trans. Aerosp. Electron. Syst.*, vol. AES-24, no. 4, pp. 427–445, Jul. 1988.
[15] M. O. Ulfarsson and V. Solo, "Dimension estimation in noisy PCA with SURE and random matrix theory," *IEEE Trans. Signal Process.*, vol. 56, no. 12, pp. 5804–5816, Dec. 2008.
[16] H. Cox and R. Pitre, "Robust DMR and multi-rate adaptive beamforming," in *Proc. Conf. Rec. 31st Asilomar Conf. Signals, Syst. Comput.*, Pacific Grove, CA, USA, vol. 1, Nov. 1997, pp. 920–924.
[17] J. R. Buck and K. E. Wage, "A random matrix theory model for the dominant mode rejection beamformer notch depth," in *Proc. IEEE Stat. Signal Process. Workshop (SSP)*, Ann Arbor, MI, USA, Aug. 2012, pp. 820–823.
[18] K. E. Wage and J. R. Buck, "Convergence rate of the dominant mode rejection beamformer for a single interferer," in *Proc. IEEE Int. Conf. Acoust., Speech Signal Process.*, Vancouver, BC, Canada, May 2013, pp. 3796–3800.
[19] K. E. Wage and J. R. Buck, "SINR loss of the dominant mode rejection beamformer," in *Proc. IEEE Int. Conf. Acoust., Speech Signal Process. (ICASSP)*, South Brisbane, QLD, Australia, Apr. 2015, pp. 2499–2503.
[20] E. L. Santos, M. D. Zoltowski, and M. Rangaswamy, "Indirect dominant mode rejection: A solution to low sample support beamforming," *IEEE Trans. Signal Process.*, vol. 55, no. 7, pp. 3283–3293, Jul. 2007.
[21] C. Hulbert and K. Wage, "Random matrix theory predictions of dominant mode rejection beamformer performance," *IEEE Open J. Signal Process.*, vol. 3, pp. 229–245, 2022.
[22] H. Cox, "Resolving power and sensitivity to mismatch of optimum array processors," *J. Acoust. Soc. Amer.*, vol. 54, no. 3, pp. 771–785, Sep. 1973.
[23] E. N. Gilbert and S. P. Morgan, "Optimum design of directive antenna arrays subject to random variations," *Bell Syst. Tech. J.*, vol. 34, no. 3, pp. 637–663, May 1955.
[24] S. M. Kay, *Fundamentals of Statistical Signal Processing* (Signal Processing Series). Englewood Cliffs, NJ, USA: Prentice-Hall, 1993.
[25] R. von Mises, "Über die 'ganzzahligkeit' der atomgewicht und verwandte fragen," *Physikalische Zeitschrift*, no. 19, pp. 490–500, 1918.
[26] A. Aubry, V. Carotenuto, A. Farina, and A. De Maio, "Radar phase noise modeling and effects—Part II: Pulse Doppler processors and sidelobe blankers," *IEEE Trans. Aerosp. Electron. Syst.*, vol. 52, no. 2, pp. 712–725, Apr. 2016.
[27] C. C. Hulbert and K. E. Wage, "Random matrix theory analysis of the dominant mode rejection beamformer white noise gain with overestimated rank," in *Proc. 54th Asilomar Conf. Signals, Syst., Comput.*, Pacific Grove, CA, USA, Nov. 2020, pp. 490–495.
[28] V. A. Marčenko and L. A. Pastur, "Distribution of eigenvalues for some sets of random matrices," *Math. USSR-Sbornik*, vol. 1, no. 4, pp. 457–483, Apr. 1967.
[29] Z. Bai and J. W. Silverstein, *Spectral Analysis of Large Dimensional Random Matrices*, 2nd ed. New York, NY, USA: Springer, 2010.

DAVID CAMPOS ANCHIETA received the M.S. degree in electrical engineering from the University of Massachusetts Dartmouth, in 2021, where he is currently pursuing the Ph.D. degree in electrical engineering.

JOHN R. BUCK (Senior Member, IEEE) received the Ph.D. degree in oceanographic engineering from the MIT/WHOI Joint Program, in 1996. He is currently a Chancellor Professor of electrical and computer engineering with the University of Massachusetts Dartmouth. He is a fellow of the Acoustical Society of America.